Table VI. Oxidation of Ethyl Radical by Fe^{3+}(aq) in Acetonitrile-Water Mixtures[a]

	ethyl products, mmol			
H_2O[b]	EtH	Et(-H)	EtOH	EtNHAc
0	0.16	0.09	0.51	0.30
10	0.55	0.04	0.71	trace[c]
25[d]	0.41	0.01	0.80	trace[c]

[a] Reactions carried out with 4.0 mmol of $Fe(H_2O)_6(ClO_4)_3$ and 1.0 mmol of Et_4Pb in 15 mL of solvent at 22 °C. [b] Volume %. [c] ≤0.05 mmol. [d] Et_4Pb not completely dissolved.

8 h. Ethane and ethylene were determined by gas chromatography using a 2 ft × 1/8 in. column of Porapak Q. Ethanol was analyzed on a 6 ft × 1/8 in. column of Porapak Q. A 3 ft × 1/8 in. column of FFAP was used for the analysis of *N*-ethylacetamide.

The results in Table VI indicate that ethyl radicals are readily oxidized by iron(III) in either acetonitrile or aqueous acetonitrile solutions to afford high yields of *N*-ethylacetamide and/or ethyl alcohol. Such an oxidation can proceed by either electron transfer to afford an ethyl cation or by an associative process involving an ethyliron(IV) intermediate.[38] These mechanisms bear critically on other oxidations such as those utilizing the Fenton's reagent[39] and merit further study.

Acknowledgment. We wish to thank the National Science Foundation for financial support and W. Lau for help with the spectral measurements.

Registry No. $(NC)_2Fe(phen)_2$, 15362-08-0; $CH_3NC(NC)Fe(phen)_2PF_6$, 80925-96-8; $(CH_3NC)_2Fe(phen)_2(PF_6)_2$, 49664-77-9; CH_3NC, 75-05-8; $(NC)_2Fe(phen)_2PF_6$, 80925-97-9; $Fe(H_2O)_6(ClO_4)_3$, 32963-81-8; $FeCl_4^-$, 14946-92-0; $FeCl_3$, 7705-08-0; $FeCl_2$, 7758-94-3; $FeCl_2^+$, 15905-98-3; $CH_3\cdot$, 2229-07-4; $CH_3CH_2\cdot$, 2025-56-1; $(CH_3)_2CH\cdot$, 2025-55-0; $(CH_3)3C\cdot$, 14804-25-2.

(38) At this juncture, the source of the increasing yields of ethane with water concentration is somewhat ambiguous. A reviewer has indicated that Et_4Pb does not undergo unassisted hydrolysis by water at any appreciable rate. However, the formation of ethyl alcohol and *N*-ethylacetamide does generate an equivalent of acid, which could lead to an enhanced rate of protonolysis. Alternatively, ethane may arise from the hydrolysis of a putative organoiron intermediate; as suggested by the reviewer.

(39) Walling, C. *Acc. Chem. Res.* **1975**, *8*, 125.

Cyclopentadienylcobalt 1,4-Diaryltetraazadienes. A Structural, Spectroscopic, and Theoretical Study

Michal E. Gross, William C. Trogler,* and James A. Ibers

Department of Chemistry, Northwestern University, Evanston, Illinois 60201

Received January 22, 1982

Unsaturated metallacycles such as $(\eta^5\text{-}C_5H_5)Co(R{-}N{=}N{-}N{=}N{-}R)$, where R = alkyl or aryl, offer the possibility of π-delocalized bonding. Xα calculations predict that two dπ electrons on the $(\eta^5\text{-}C_5H_5)Co$ fragment should strongly interact with an empty low-lying π^* orbital of the tetraazadiene ligand to yield metallacycle π and π^* orbitals. A single-crystal X-ray diffraction study at −150 °C of the R = C_6F_5 derivative provides direct evidence of the π-acceptor abilities of the RN_4R ligand. The Co[(N(1)N(2)N(3)N(4)] ring is planar and exhibits unusually short Co–N(1) and Co–N(4) distances of 1.802 (2) and 1.819 (2) Å, respectively, indicative of multiple-bond character. The short N(2)–N(3) bond [1.279 (2) Å] and long N(1)–N(2) [1.360 (2) Å] and N(3)–N(4) [1.355 (2) Å] bonds demonstrate that π back-bonding has altered the pattern of unsaturated bonds in the tetraazadiene chelate. Electronic absorption spectra of $(\eta^5\text{-}C_5H_5)Co(RN_4R)$ [R = CH_3, C_6H_5, C_6F_5, 2,4-$F_2C_6H_3$, 2,6-$(CH_3)_2C_6H_3$] display three bands characteristic of the cobalt–tetraazadiene ring: λ_{max}^1 (ϵ), 600–670 nm (300–700); λ_{max}^2 (ϵ), 425–470 nm (5000–9000); λ_{max}^3 (ϵ), 335–390 nm (<4000). These absorptions are attributed to one-electron transitions that terminate in the low-lying metallacycle π^* orbital. Crystals of $C_{17}H_5CoF_{10}N_4\cdot{}^1/_2C_6H_6$ at −150 °C are monoclinic, space group $P2_1/c$, with four formula units in a cell of dimensions a = 8.612 (4) Å, b = 22.687 (12) Å, c = 9.820 (6) Å, and β = 91.58 (2)°. Least-squares refinement of 315 variables has led to a final value of the R index on F^2 of 0.047 for 5367 observations; the conventional R index on F is 0.033 for 4313 observations having $F_o^2 > 3\sigma(F_o^2)$.

Introduction

Partially occupied π orbitals on a metal atom and unsaturated chelate permit the formulation of a $(4n + 2)$ π-electron ring. Six electron systems such as I, where M

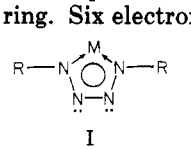

I

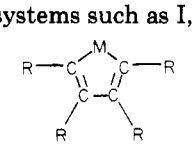

II

is $(\eta^5\text{-}C_5H_5)Co$, $Fe(CO)_3$, or some other d^8 moiety have attracted our attention.[1,2] The available structural data for metallacyclopentadiene complexes, MC_4R_4 (II), indicate little delocalization of the π-electron system;[3] extended Hückel molecular orbital calculations support these observations.[4] Delocalized electronic structures have been proposed for heterocycles of the type $MC_2R_2X_2$, X = S, NR′ (III), on the basis of structure determinations and spectroscopic data.[5,6] Further heteroatom substitution

(1) (a) Gross, M. E.; Trogler, W. C.; Ibers, J. A. *J. Am. Chem. Soc.* **1981**, *103*, 192–193. (b) Gross, M. E.; Trogler, W. C. *J. Organomet. Chem.* **1981**, *209*, 407–414. (c) Gross, M. E.; Ibers, J. A.; Trogler, W. C., *Organomet.*, in press. (d) Gross, M. E.; Trogler, W. C., submitted for publication.

(2) (a) Trogler, W. C.; Johnson, C. E.; Ellis, D. E. *Inorg. Chem.* **1981**, *20*, 980–986. (b) Johnson, C. E.; Trogler, W. C. *J. Am. Chem. Soc.* **1981**, *103*, 6352–6358. (c) Johnson, C. E.; Trogler, W. C. *Inorg. Chem.*, **1981**, *21*, 427–429. (d) Chang, C.-Y.; Johnson, C. E.; Richmond, T. G.; Chen, Y.-T.; Trogler, W. C.; Basolo, F. *Ibid* **1981**, *20*, 3167–3172.

(3) See, for example: (a) Suzuki, H.; Itoh, K.; Ishii, Y.; Simon, K.; Ibers, J. A. *J. Am. Chem. Soc.* **1976**, *98*, 8494–8500 and references therein. (b) Yamazaki, H.; Wakatsuki, Y. *J. Organomet. Chem.* **1977**, *139*, 157–167. (c) Collman, J. P.; Kang, J. W.; Little, W. F.; Sullivan, M. F. *Inorg. Chem.* **1968**, *7*, 1298–1303.

(4) Thorn, D. L.; Hoffmann, R. *Nouv. J. Chim.* **1979**, *3*, 39–45.

0276-7333/82/2301-0732$01.25/0

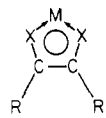

III

of $MC_2R_2N_2$ yields the nitrogen-based metallatetraazadiene complexes, MN_4R_2 (I), which have received surprisingly little attention.[7-14] Complete π delocalization in the metallatetraazadiene moiety, as reflected by equalization of the N–N bonds, might follow a pattern of greater delocalization with increasing heteroatom substitution. The remarkable thermal stability of d^8 metallatetraazadiene complexes (the metal-free tetraazadiene molecule is not known) may be one consequence of such delocalization. The few structural determinations of metallatetraazadienes exhibit differing degrees of π-bond delocalization.[8,9,12] The RN_4R chelates in complexes of type I belong to a class of suspect ligands that may assume configurations ranging from the 1,3-diene, as in structure 1, to the reduced 2-ene, as in structure 2.

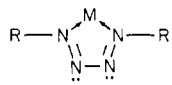

1

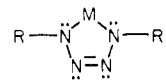

2

Experimental Section

The complexes $(\eta^5\text{-}C_5H_5)Co(RN_4R)$, R = CH_3 (IVa), C_6H_5 (IVb), C_6F_5 (IVc), 2,4-$F_2C_6H_3$ (IVd), 2,6-$(CH_3)_2C_6H_3$ (IVe), were prepared from $(\eta^5\text{-}C_5H_5)Co(CO)_2$ and RN_3 by previously described procedures.[1b,d,14] Absorption spectra were recorded at room temperature in solution and at 77 K in 2-methylpentane glasses on a Perkin-Elmer 320 spectrophotometer. Dark green crystals, suitable for X-ray diffraction study, were grown by slow evaporation of a benzene solution of IVc.

X-ray Data Collection for $(\eta^5\text{-}C_5H_5)Co(C_6F_5N_4C_6F_5)\cdot{}^1/_2C_6H_6$. Preliminary room-temperature X-ray photographic data showed the crystal to be monoclinic with systematic extinctions ($h0l$, $l = 2n + 1$; $0k0$, $k = 2n + 1$) consistent with the space group C_{2h}^5—$P2_1/c$.

Data collection was carried out on a four-circle, computer-controlled Picker FACS-1 diffractometer with the crystal at −150 °C.[15] The crystal of rectangular prismatic habit had the eight faces {110}, {010}, and {001}, with distances between members of the forms of 0.348, 0.372, 0.464, and 0.740 mm and a volume of 0.102 mm^3. Unit-cell dimensions were determined by a least-squares analysis of the angular positions of 15 hand-centered reflections[16] at −150 °C in diverse regions of reciprocal space (25° $\leq 2\theta(\text{Mo K}\alpha_1) \leq 34°$). The complex $C_{17}H_5CoF_{10}N_4\cdot{}^1/_2C_6H_6$, molecular weight 553.23 amu, crystallizes at −150 °C with four formula units in a cell of dimensions a = 8.612 (4) Å, b = 22.687 (12) Å, c = 9.820 (6) Å, β = 91.58(2)°, V = 1918 $Å^3$, ρ_{obsd} = 1.71 (2) g/cm^3 (25 °C), and ρ_{calcd} = 1.796 g/cm^3 (−150 °C).

Data collection was carried out by using techniques standard in this laboratory,[16] employing monochromatized Mo Kα radiation (λ(Mo Kα_1) = 0.709 30 Å). Intensities for reflections $\pm h,+k,+l$ were measured in the range $3.5° \leq 2\theta \leq 59°$. A scan speed of 2°/min in 2θ ranging from 1.5° below Kα_1 to 1.0° above Kα_2 for $3.5° \leq 2\theta \leq 33°$ and 1.1° below Kα_1 to 1.0° above Kα_2 for $2\theta > 33°$ was employed. The takeoff angle was 3.2°. Of the 5367 unique reflections collected, 4313 had $F_o^2 > 3\sigma(F_o^2)$. An absorption correction was applied to the data with the use of an absorption coefficient of 9.4 cm^{-1}; resultant transmission factors fell in the range 0.659–0.741.

Solution and Refinement of the Structure. The cobalt atom was located readily from an origin-removed Patterson synthesis, and all remaining nonhydrogen and hydrogen atoms were located by Fourier methods. The usual procedure for refinement was employed.[17]

The benzene solvate, located at an inversion center $(0,{}^1/_2,0)$, was treated throughout as a planar rigid body with uniform C–C distances of 1.392 Å and idealized D_{6h} symmetry. The positions of the hydrogen atoms of the benzene solvate were determined from a C–H distance of 1.00 Å. The function $\sum w(F_o^2 - F_c^2)^2$ was minimized in the final cycle of refinement, in which all nonhydrogen atoms of the metal complex were refined anisotropically and the cyclopentadienyl hydrogen atoms isotropically. This refinement involved 315 variables and 5367 observations (including those for which $F_o^2 < 0$). It converged to values of R and R_w (on F_o^2) of 0.047 and 0.086, respectively, to an error in an observation of unit weight of 1.43 electrons,[2] and for those reflections having $F_o^2 > 3\sigma(F_o^2)$ to values of the conventional R and R_w indices on $|F_o|$ of 0.033 and 0.043, respectively. A final difference electron density map revealed no peaks above 0.7 $e/Å^3$ except for one ripple (0.81 $e/Å^3$) within 0.9 Å of the cobalt atom. The positional parameters are listed in Table I. The thermal parameters, root-mean-square amplitudes of vibration, and a tabulation of the observed and calculated structure amplitudes are available.[18]

Xα Calculations. Computations employed the SCC-DV-Xα method. The Hartree–Fock–Slater equations were solved iteratively by the discrete variational (DV) procedure,[19] and the Coulomb potential was approximated by an S-wave potential from the population-charge analysis.[20] An Xα exchange parameter of 0.70 was assumed to avoid empiricism. Numerical atomic orbitals from exact atomic HFS calculations were used as basis functions, and core electrons were included with no further approximation.

The experimental geometry of IVc was idealized to C_s symmetry (mirror plane perpendicular to CoN_4 plane and bisecting the NCoN angle). The C_6F_5 groups were replaced by H atoms (N–H distance assumed to be 1.01 Å). In the comparative calculation of $Fe(CO)_3(HN_4H)$ we assumed the same HN_4H configuration as in the cobalt complex. The $Fe(CO)_3$ geometry was that used in a previous study.[2a]

Results and Discussion

Description of the Structure of $(\eta^5\text{-}C_5H_5)Co(C_6F_5N_4C_6F_5)\cdot{}^1/_2C_6H_6$. The crystal structure of $(\eta^5\text{-}C_5H_5)Co(C_6F_5N_4C_6F_5)\cdot{}^1/_2C_6H_6$ consists of the packing of four molecules of the cobalt complex and two benzene molecules in the unit cell (Figure 1). The labeling scheme for the cobalt complex is presented in Figure 2; selected bond distances and angles are given in Figure 3 and Table II. The complex, excluding the phenyl substituents, ex-

(5) (a) Schrauzer, G. N. *Acc. Chem. Res.* **1969**, *2*, 72–80. (b) McCleverty, J. A. *Prog. Inorg. Chem.* **1968**, *10*, 49–221. (c) Shupack, S. I.; Billig, E.; Clark, R. J. H.; Williams, R.; Gray, H. B. *J. Am. Chem. Soc.* **1964**, *86*, 4594–4602.

(6) (a) Krumholz, P. *Struct. Bonding (Berlin)* **1971**, *9*, 139–174. (b) Bayer, E. *Angew. Chem., Int. Ed. Engl.* **1964**, *3*, 325–332. (c) Figgins, P. E.; Busch, D. H. *J. Am. Chem. Soc.* **1960**, *82*, 820–824.

(7) Dekker, M.; Knox, G. R. *Chem. Commun.* **1967**, 1243–1244.

(8) Doedens, R. J. *Chem. Commun.* **1968**, 1271–1272.

(9) Einstein, F. W. B.; Sutton, D. *Inorg. Chem.* **1972**, *11*, 2827–2831.

(10) Ashley-Smith, J.; Green, M.; Stone, F. G. A. *J. Chem. Soc., Dalton Trans.* **1971**, 1805–1809.

(11) Cenini, S.; Fantucci, P.; La Monica, G. *Inorg. Chim. Acta* **1975**, *13*, 243–245. La Monica, G.; Sandrini, P.; Zingales, Z.; Cenini, S. *J. Organomet. Chem.* **1973**, *50*, 287–296. Beck, W.; Bauder, M.; La Monica, G.; Cenini, S.; Ugo, R. *J. Chem. Soc. A* **1971**, 113–118.

(12) Overbosch, P.; van Koten, G.; Overbeek, O. *J. Am. Chem. Soc.* **1980**, *102*, 2091–2093.

(13) Overbosch, P.; van Koten, G.; Vrieze, K. *J. Organomet. Chem.* **1981**, *208*, C21–C24.

(14) Otsuka, S.; Nakamura, A. *Inorg. Chem.* **1968**, *7*, 2542–2544.

(15) The design of the low-temperature apparatus is from: Huffman, J. C., Ph.D. Thesis, Indiana University, 1974.

(16) Corfield, P. W. R.; Doedens, R. J.; Ibers, J. A. *Inorg. Chem.* **1967**, *6*, 197–204.

(17) See for example: Waters, J. M.; Ibers, J. A. *Inorg. Chem.* **1977**, *16*, 3273–3277.

(18) Supplementary material.

(19) Ellis, D. E.; Painter, G. H. *Phys. Rev. B* **1970**, *2*, 2887–2898.

(20) Ellis, D. E.; Rosen, A.; Adachi, H.; Averill, F. W. *J. Chem. Phys.* **1976**, *65*, 3629–3634.

Table I. Positional Parameters for the Atoms of $(\eta^5\text{-}C_5H_5)Co(C_6F_5N_4C_6F_5)\cdot{}^1/_2C_6H_6$

ATOM	X[A]	Y	Z	ATOM	X	Y	Z
CO	0.092437(27)	0.342974(11)	0.376382(24)	C(23)	0.40081(24)	0.478800(92)	0.76624(21)
N(1)	-0.10691(18)	0.325914(72)	0.41121(16)	C(24)	0.33063(23)	0.430065(88)	0.82046(19)
N(2)	-0.16969(19)	0.348553(81)	0.52549(17)	C(25)	0.21928(23)	0.400008(82)	0.74478(19)
N(3)	-0.07300(19)	0.380659(81)	0.59330(18)	C(26)	0.17572(21)	0.416873(81)	0.61291(19)
N(4)	0.06626(18)	0.384279(70)	0.53284(16)	F(11)	-0.30837(15)	0.368676(53)	0.20713(13)
C(1)	0.25018(22)	0.376646(88)	0.24355(19)	F(12)	-0.50802(14)	0.297673(61)	0.06777(12)
C(2)	0.14209(22)	0.339406(88)	0.17257(19)	F(13)	-0.52467(14)	0.181879(60)	0.13110(13)
C(3)	0.15128(22)	0.282854(87)	0.23203(19)	F(14)	-0.33392(15)	0.135638(55)	0.32716(14)
C(4)	0.26455(22)	0.284675(91)	0.34042(21)	F(15)	-0.12877(14)	0.205610(54)	0.46381(13)
C(5)	0.32636(21)	0.342902(92)	0.34639(20)	F(21)	0.20947(17)	0.486037(55)	0.43517(12)
C(11)	-0.31178(21)	0.311106(85)	0.23742(19)	F(22)	0.42613(16)	0.544855(57)	0.58359(14)
C(12)	-0.41503(21)	0.275409(94)	0.16639(19)	F(23)	0.50887(16)	0.508300(63)	0.83851(14)
C(13)	-0.42247(21)	0.216304(92)	0.19772(20)	F(24)	0.36861(16)	0.412239(60)	0.94644(12)
C(14)	-0.32573(22)	0.192972(85)	0.29756(20)	F(25)	0.15528(15)	0.352167(52)	0.80026(12)
C(15)	-0.22229(21)	0.229013(85)	0.36693(19)	H(1)	0.2626(30)	0.4193(11)	0.2290(27)
C(16)	-0.21347(20)	0.288999(83)	0.33899(18)	H(2)	0.0753(32)	0.3538(11)	0.0985(29)
C(21)	0.24756(24)	0.466466(86)	0.56150(20)	H(3)	0.0843(29)	0.2476(11)	0.2052(26)
C(22)	0.35898(25)	0.497280(92)	0.63686(22)	H(4)	0.2886(31)	0.2521(11)	0.4017(27)
C(31)	0.08023(16)	0.520868(64)	0.115183(78)	H(5)	0.4023(30)	0.3575(11)	0.4134(27)
C(33)	0.03323(17)	0.522325(64)	-0.127979(58)	H(31)	0.13787(27)	0.53586(11)	0.19798(13)
C(35)	-0.11346(14)	0.456807(53)	0.01280(13)	H(33)	0.05710(30)	0.53836(11)	-0.21997(10)
				H(35)	-0.19497(24)	0.425777(92)	0.02199(23)

[A] ESTIMATED STANDARD DEVIATIONS IN THE LEAST SIGNIFICANT FIGURE(S) ARE GIVEN IN PARENTHESES IN THIS AND ALL SUBSEQUENT TABLES.

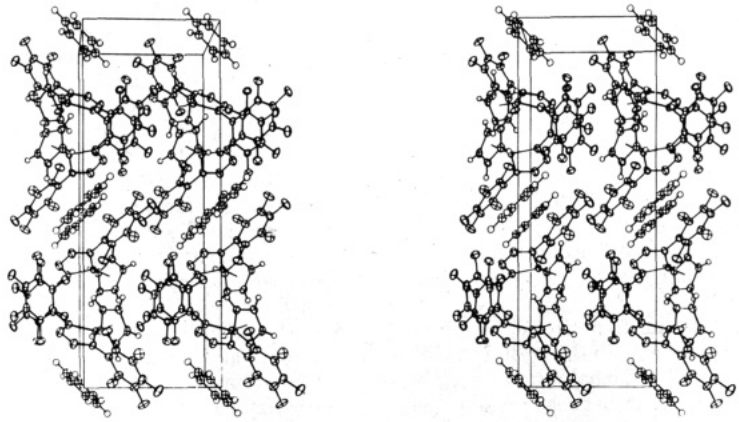

Figure 1. Stereoview of the unit cell of $(\eta^5\text{-}C_5H_5)Co(C_6F_5N_4C_6F_5)\cdot{}^1/_2C_6H_6$. The *b* axis is almost vertical, and the *a* axis is horizontal to the right. Vibrational ellipsoids are drawn at the 50% probability level; hydrogen atoms are drawn at the 20% probability level for clarity.

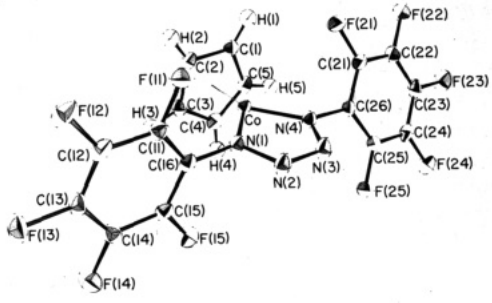

Figure 2. Drawing of an individual molecule of $(\eta^5\text{-}C_5H_5)Co(C_6F_5N_4C_6F_5)$ (IVc) showing the labeling scheme. Vibrational ellipsoids are drawn at the 50% probability level.

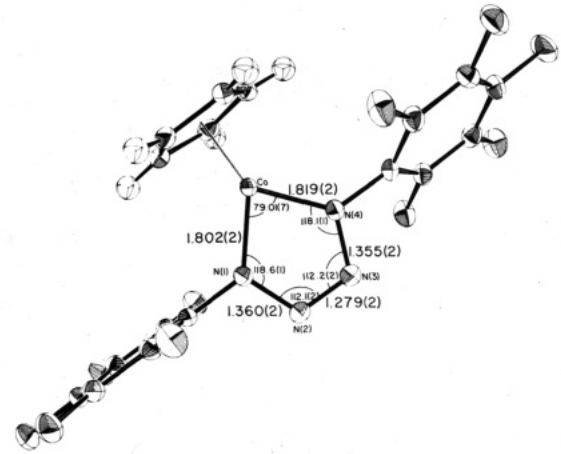

Figure 3. Selected bond distances (Å) and bond angles (deg) for the metallatetraazadiene moiety of $(\eta^5\text{-}C_5H_5)Co(C_6F_5N_4C_6F_5)$ (IVc). Vibrational ellipsoids are drawn at the 50% probability level.

hibits virtual $C_s(m)$ symmetry, with a mirror plane perpendicular to the metallacycle and cyclopentadienyl planes and bisecting the N(1)–Co–N(4) and C(3)–C(4)–C(5) angles. The geometry about the cobalt atom, which is co-

Table II. Intramolecular Bond Distances (Å) and Angles (Deg) in $(\eta^5\text{-}C_5H_5)Co(C_6F_5N_4C_6F_5)\cdot{}^1/_2C_6H_6$

Bond Distances

Co-N(1)	1.802 (2)	1.811 (12)[a]	C(16)-C(11)	1.384 (3)	
Co-N(4)	1.819 (2)		C(11)-C(12)	1.378 (3)	
N(1)-N(2)	1.360 (2)		C(12)-C(13)	1.378 (3)	1.380 (6)
N(2)-N(3)	1.279 (2)		C(13)-C(14)	1.375 (3)	
N(3)-N(4)	1.355 (2)		C(14)-C(15)	1.376 (3)	
N(1)-C(16)	1.418 (2)		C(15)-C(16)	1.391 (3)	
N(4)-C(26)	1.419 (2)		C(11)-F(11)	1.340 (2)	
Co-C(1)	2.056 (2)		C(12)-F(12)	1.338 (2)	
Co-C(2)	2.060 (2)		C(13)-F(13)	1.335 (2)	
Co-C(3)	2.041 (2)	2.045 (14)	C(14)-F(14)	1.335 (2)	
Co-C(4)	2.025 (2)		C(15)-F(15)	1.339 (2)	1.337 (2)
Co-C(5)	2.044 (2)		C(21)-F(21)	1.341 (2)	
C(1)-C(2)	1.425 (3)		C(22)-F(22)	1.338 (2)	
C(2)-C(3)	1.411 (3)		C(23)-F(23)	1.335 (2)	
C(3)-C(4)	1.424 (3)	1.420 (7)	C(24)-F(24)	1.334 (2)	
C(4)-C(5)	1.425 (3)		C(25)-F(25)	1.340 (2)	
C(5)-C(1)	1.414 (3)		C(26)-C(21)	1.386 (3)	
C(1)-H(1)	0.98 (3)		C(21)-C(22)	1.385 (3)	
C(2)-H(2)	0.97 (3)		C(22)-C(23)	1.376 (3)	
C(3)-H(3)	1.02 (3)	0.98 (3)	C(23)-C(24)	1.374 (3)	1.382 (7)
C(4)-H(4)	0.97 (3)		C(24)-C(25)	1.378 (3)	
C(5)-H(5)	0.97 (3)		C(25)-C(26)	1.392 (3)	

Bond Angles

N(1)-Co-N(4)	79.01 (7)	N(1)-C(16)-C(11)	121.4 (2)	F(11)-C(11)-C(16)	119.8 (2)
Co-N(1)-N(2)	118.6 (1)	N(1)-C(16)-C(15)	121.2 (2)	F(11)-C(11)-C(12)	118.6 (2)
Co-N(4)-N(3)	118.1 (1)	C(15)-C(16)-C(11)	117.5 (2)	F(12)-C(12)-C(11)	120.6 (2)
N(1)-N(2)-N(3)	112.1 (2)	C(16)-C(11)-C(12)	121.7 (2)	F(12)-C(12)-C(13)	119.9 (2)
N(2)-N(3)-N(4)	112.2 (2)	C(11)-C(12)-C(13)	119.5 (2)	F(13)-C(13)-C(12)	119.6 (2)
Co-N(1)-C(16)	129.7 (1)	C(12)-C(13)-C(14)	120.2 (2)	F(13)-C(13)-C(14)	120.2 (2)
Co-N(4)-C(26)	129.8 (1)	C(13)-C(14)-C(15)	119.7 (2)	F(14)-C(14)-C(13)	119.7 (2)
N(2)-N(1)-C(16)	111.7 (1)	C(14)-C(15)-C(16)	121.5 (2)	F(14)-C(14)-C(15)	120.6 (2)
N(3)-N(4)-C(26)	111.8 (2)	N(4)-C(26)-C(21)	121.2 (2)	F(15)-C(15)-C(14)	119.0 (2)
C(5)-C(1)-C(2)	108.2 (2)	N(4)-C(26)-C(25)	122.0 (2)	F(15)-C(15)-C(16)	119.5 (2)
C(1)-C(2)-C(3)	108.0 (2)	C(25)-C(26)-C(21)	116.8 (2)	F(21)-C(21)-C(26)	118.1 (2)
C(2)-C(3)-C(4)	108.2 (2)	C(26)-C(21)-C(22)	121.7 (2)	F(21)-C(21)-C(22)	118.1 (2)
C(3)-C(4)-C(5)	107.8 (2)	C(21)-C(22)-C(23)	120.0 (2)	F(22)-C(22)-C(21)	119.9 (2)
C(4)-C(5)-C(1)	107.9 (2)	C(22)-C(23)-C(24)	119.7 (2)	F(22)-C(22)-C(23)	120.1 (2)
		C(23)-C(24)-C(25)	119.8 (2)	F(23)-C(23)-C(22)	119.9 (2)
		C(24)-C(25)-C(26)	122.1 (2)	F(23)-C(23)-C(24)	120.3 (2)
				F(24)-C(24)-C(23)	120.3 (2)
				F(24)-C(24)-C(25)	120.0 (2)
				F(25)-C(25)-C(24)	118.0 (2)
				F(25)-C(25)-C(26)	119.8 (2)

[a] The figure in parentheses following an average value is the larger of that estimated for an individual value from the matrix or on the assumption that the values averaged are from the same population.

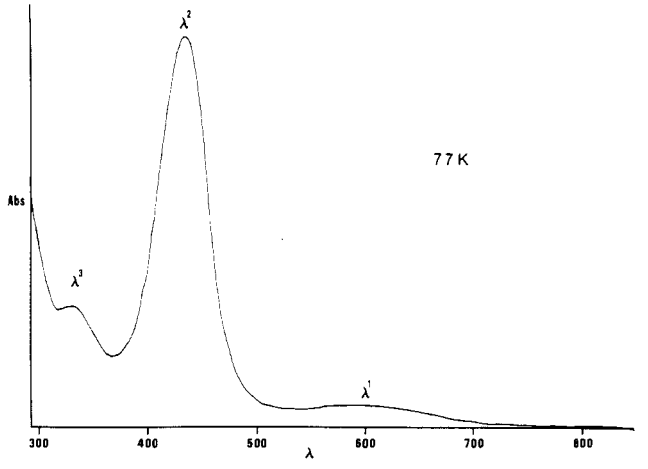

Figure 4. Electronic absorption spectrum of $(\eta^5\text{-}C_5H_5)Co(CH_3N_4CH_3)$ at 77 K in a 2-methylpentane glass.

ordinated to the cyclopentadienyl ring and the terminal nitrogen atoms, N(1) and N(4), is trigonal. The cyclopentadienyl ligand is symmetrically disposed with respect to the metallacycle plane, forming a dihedral angle of 85.56°.

Structural Aspects of the Metallacycle. Consider the remarkably stable metallatetraazadiene moiety. The CoN_4 ring is planar with the largest deviation of an atom from the least-squares plane of the ring being 0.014 (2) Å (Table III). The Co–N(1) and Co–N(4) bond lengths of 1.802 (2) and 1.819 (2) Å, respectively, are the shortest known M–N distances of any tetraazadiene complex (Table IV). These distances indicate multiple bonding, as M–N single bonds would fall in the range 1.95–2.15 Å.[21] Inequivalence of the N–N bond lengths rules out balanced delocalization of π bonding in the metallacycle; partial delocalization, however, is consistent with the observed data. The central, N(2)–N(3) bond [1.279(2) Å] is longer than that found in tetrakis(trimethylsilyl)tetrazene, V,

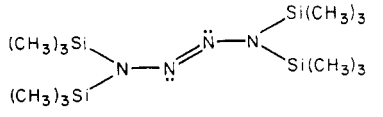

V

[1.268 (7) Å][22] and still longer than the sum of the nitrogen

(21) Davis, B. R.; Payne, N. C.; Ibers, J. A. *Inorg. Chem.* **1969**, *8*, 2719–2728.

Table III. Least-Squares Planes in $(\eta^5\text{-}C_5H_5)Co(C_6F_5N_4C_6F_5)$

plane no.	description	plane equations: $Ax + By + Cz = D$[a] A	B	C	D	dev from plane,[b] Å
1	metallatetraazadiene	2.499	−18.105	5.106	−4.057	Co, 0.000 (1); N(1), −0.011 (2); N(2), 0.006 (2); N(3), 0.012 (2); N(4), −0.014 (2)
2	phenyl 1	6.114	−4.224	−6.860	−4.848	C(11), −0.001 (2); C(12), 0.006 (2); C(13), −0.005 (2); C(14), 0.000 (2); C(15), 0.004 (2); C(16), −0.004 (2)
3	phenyl 2	6.235	−13.189	−3.840	−6.763	C(21), −0.003 (2); C(22), −0.004 (2); C(23), 0.004 (2); C(24), 0.001 (2); C(25), −0.006 (2); C(26), 0.006 (2)
4	cyclopentadienyl carbon atoms	6.239	−5.831	−6.475	−2.210	C(1), −0.002 (2); C(2), 0.000 (2); C(3), 0.002 (2); C(4), −0.004 (2); C(5), 0.004 (2); Co, −1.650; H(1), −0.079; H(2), −0.021; H(3), −0.037; H(4), −0.061; H(5) −0.041
5	cyclopentadienyl hydrogen atoms	6.28	−5.74	−6.44	−2.21	H(1), −0.02 (3); H(2), 0.02 (3); H(3), 0.00 (3); H(4), −0.01 (3); H(5), 0.02 (3); Co, −1.60; C(1), 0.05; C(2), 0.04; C(3), 0.04; C(4), 0.04; C(5), 0.06

Interplanar Angles, Deg

plane no.	plane no.	angle	plane no.	plane no.	angle
1	2	90.24	2	3	29.03
1	3	61.45	2	4	4.72
1	4	85.56	3	4	24.31
			4	5	0.40

[a] Equations of planes are expressed in crystal coordinates as defined by: Hamilton, W. C. *Acta Crystallogr.* **1961**, *14*, 185–189. [b] Standard deviations are given for those atoms used in the definition of a particular plane.

Table IV. Comparison of Metallatetraazadiene Bond Distances (Å)

		M-N(av)	$N_{1,4}$-$N_{2,3}$(av)	N_2-N_3	N-C(phenyl)(av)
IVc	$(\eta^5\text{-}C_5H_5)Co(C_6F_5N_4C_6F_5)$[a]	1.811 (8)[b]	1.358 (3)	1.279 (2)	1.419 (2)
VI	$Ni(RN_4R)_2$ R = 3,5-$(CH_3)_2C_6H_3$[c]	1.853 (3)	1.325 (3)	1.319 (4)	1.426 (4)
VII	$Fe(CO)_3(CH_3N_4CH_3)$[d]	1.85 (3)	1.31 (7)	1.30 (7)	
VIII	$[Ir(CO)(P(C_6H_5)_3)_2(RN_4R)][BF_4]$[e] R = *p*-$FC_6H_4$	1.956 (15)	1.375 (25)	1.270 (16)	1.469 (18)

[a] This work at −150 °C. All other structural data tabulated here were obtained at room temperature. [b] The standard deviation in parentheses following the average value for bond lengths of the same type in a given complex is the larger of that estimated for an individual value from the inverse matrix or on the assumption that the values averaged are from the same population. [c] Reference 12. [d] Reference 8. [e] Reference 9.

covalent double bond radii (1.24 Å).[23] Conversely, the terminal N(1)–N(2) [1.360 (2) Å] and N(3)–N(4) [1.355 (2) Å] bond lengths are much shorter than the corresponding bonds in V [1.394 (5) Å] and the sum of the nitrogen covalent single-bond radii (1.40 Å). These data support the importance of the resonance forms **3** or **4**. However, no simple valence-bond description adequately represents the observed structure.

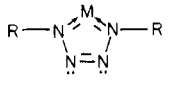

3

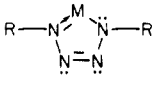

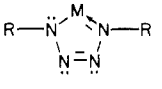

4

The pentafluorophenyl rings are not coplanar with the metallatetraazadiene plane; the C_6 rings form dihedral angles of 90.24° and 61.45° with the CoN_4 plane. Differing degrees of conjugation between the unsaturated metallacycle and each of the phenyl rings may account for the significant (>6σ) inequivalence of the Co–N bond lengths.

A larger π interaction between atom N(4) and its phenyl ring (phenyl 2 of Table III) is expected as a result of the smaller dihedral angle (61.45°). This would weaken the Co–N(4) π interaction, as reflected in the longer bond length relative to the Co–N(1) distance. Note that the N–C(phenyl) bond lengths of complex I [1.418 (2), 1.419 (2) Å] are approximately equal to those of the complex $Ni(RN_4R)_2$, R = 3,5-$(CH_3)_2C_6H_3$ (VI) [1.426 (4) Å].[12] The NiN_4 and C_6 rings of the latter are coplanar, and strong conjugation between them has been proposed. The electron-withdrawing fluorine substituents in complex IVc must also be considered as contributing to the shortening of the N–C bonds; therefore conclusions regarding the relative degrees of conjugation in these complexes are tenuous.

The planar metallatetraazadiene moiety of $Ni(RN_4R)_2$, R = 3,5-$(CH_3)_2C_6H_3$, exhibits short M–N and equivalent N–N bond lengths (Table IV).[12] Overbosch et al. propose the diene resonance form **1**, suggesting that strong conjugation with the coplanar phenyl groups leads to equivalent N–N bond lengths. The structure of the first known metallatetraazadiene complex, $Fe(CO)_3(CH_3N_4CH_3)$, (VII),[8] which is isoelectronic with complex IVc, exhibits features similar to complex VI, including a planar metallacycle, short M–N and equivalent N–N bond lengths; however, large standard deviations of the bond lengths preclude a clear interpretation.

(22) Veith, M. *Acta Crystallogr., Sect. B* **1975**, *B31*, 678–684. An interesting comparison is with the N=N distance of 1.291 (6) Å in dimethylcyclotetrazenoborane, where extensive delocalization of the π electrons in the N_4B ring was suggested. See: Chang, C. H.; Porter, R. F.; Bauer, S. H. *Inorg. Chem.* **1969**, *8*, 1677–1683.

(23) Pauling, L. "The Nature of the Chemical Bond"; Cornell University Press: New York, 1960.

A tetrazolium-like structure, shown below, has been proposed for the iridium tetraazadiene complex $[Ir(CO)(P(C_6H_5)_3)_2(RN_4R)][BF_4]$, R = *p*-$FC_6H_4$ (VIII).[9] The N–N bond lengths

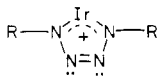

(Table IV) are similar to those of complex IVc; however, the Ir–N distances are in the single-bond range, and the Ir atom is displaced 0.12 Å out of the N_4 plane. Steric congestion may be a factor in determining the disposition of the phenyl rings, as they form dihedral angles of 66° and 49° with the N_4 plane.

That the structurally characterized metallatetraazadiene complexes exhibit localized diene and ene, as well as completely delocalized metallacycles attests to the flexible and extremely stable nature of this moiety.

Structural Aspects of the Cyclopentadienyl Ring. The five-carbon ring of the cyclopentadienyl ligand in complex IVc is essentially planar and nearly symmetrically disposed with respect to the metallatetraazadiene plane. A symmetric tilt of the C_5 ring, such that atom C(4) is closest to the cobalt atom, is evident from differences in the Co–C distances; a dihedral angle of 85.6° between the cyclopentadienyl and metallatetraazadiene planes results. Steric congestion between the cyclopentadienyl and phenyl groups, if important, should have resulted in an asymmetric tilt, owing to the different cyclopentadienyl–perfluorophenyl dihedral angles of 4.72 and 24.31°. Variations in the C–C bond lengths of the cyclopentadienyl ring are at the threshold of significance; yet they are consistent with a distortion toward a diene configuration. The origins and significance of cyclopentadienyl ligand distortions have been discussed in detail elsewhere.[1c,24-33] The distortion observed in complex IVc may result from interaction of the cyclopentadienyl moiety with a metal fragment lacking cylindrical symmetry. Differential occupation of the degenerate highest occupied molecular orbitals of the cyclopentadienyl moiety, e_1^+ and e_1^-, by nondegenerate metal d orbitals may result in diene and allyl-ene distortions, respectively.

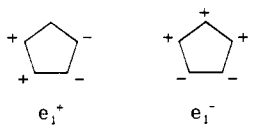

Although displacements of H atoms from the cyclopentadienyl C_5 plane are small, there is a trend of bending toward the Co atom, which is 1.602 Å from the center of the H_5 plane and 1.650 Å from the center of the C_5 plane. Similar deviations toward the metal atom have been documented for other cyclopentadienyl complexes.[1c,34-36] Complexes containing coordinated pentamethylcyclopentadienyl ligands frequently exhibit bending of the methyl substituents away from the metal atom.[25,26,37] Explanations have been proposed for C-H bending.[38,39] While the nonplanarity of the ring substituents may serve as an indicator of the electronic interactions with the metal atom, there is as yet no meaningful correlation among the limited number of accurately documented cases.

Table V. Electronic Absorption Spectral Data (nm) for $(\eta^5\text{-}C_5H_5)Co(RN_4R)$ Complexes

R	solvent	λ_{max}^1 (ϵ)	λ_{max}^2 (ϵ)	λ_{max}^3 (ϵ)
CH_3	C_6H_6	598 (260)	424 (9260)	334 (<2200)[a]
C_6H_5	$C_6H_5CH_3$	671 (690)	470 (6200)	388 (<3200)
	CH_3OH	658 (670)	468 (6880)	384 (<3600)
C_6F_5	$C_6H_5CH_3$	657 (430)	470 (5190)	346 (<2700)
	CH_3OH	650 (440)	465 (5740)	337 (<2900)
2,4-$F_2C_6H_3$	$C_6H_5CH_3$	658 (650)	466 (7430)	362 (<4000)
2,6-$(CH_3)_2C_6H_3$	C_6H_6	635 (280)	443 (5160)	341 (<2800)

[a] $\lambda_{max}3$ appears as a shoulder of an intense ultraviolet absorption band; hence extinction coefficients are approximate values.

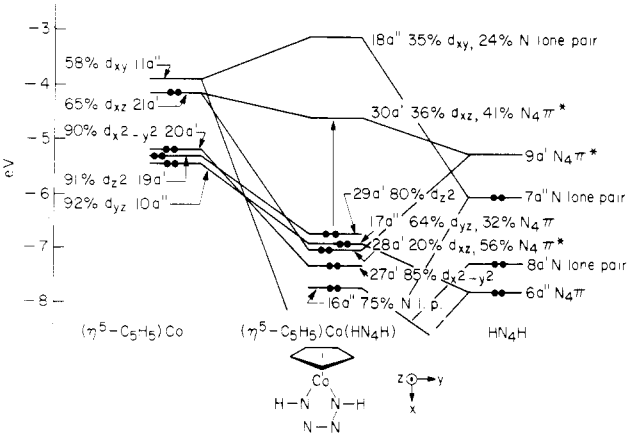

Figure 5. Orbital energy diagrams from SCC-DV-Xα calculations of the $(\eta^5\text{-}C_5H_5)Co$ and HN_4H fragments as well as of the $(\eta^5\text{-}C_5H_5)Co(HN_4H)$ molecule (C_s symmetry). The orientation of the metal coordinate system is defined at the bottom of the figure.

Electronic Spectra. The electronic spectra of complexes $(\eta^5\text{-}C_5H_5)Co(RN_4R)$ (R = CH_3, C_6H_5, C_6F_5, 2,4-$F_2C_6H_3$, 2,6-$(CH_3)_2C_6H_3$) are characterized by three low-energy electronic transitions (Figure 4, Table V). Visible absorption bands result from transitions involving primarily the metallatetraazadiene moiety; the complex $(\eta^5\text{-}C_5H_5)Co(CO)_2$ exhibits no absorption bands in the

(24) Byers, L. R.; Dahl, L. F. *Inorg. Chem.* **1980**, *19*, 277–284.
(25) Freyberg, D. P.; Robbins, J. L.; Raymond, K. N.; Smart, J. C. *J. Am. Chem. Soc.* **1979**, *101*, 892–897.
(26) Mingos, D. M. P.; Minshall, P. C.; Hursthouse, M. B.; Malik, K. M. A.; Willoughby, S. D. *J. Organomet. Chem.* **1979**, *181*, 169–182.
(27) Rigby, W.; Lee, H.-B.; Bailey, P. M.; McCleverty, J. A.; Maitlis, P. M. *J. Chem. Soc., Dalton Trans.* **1979**, 387–394.
(28) Byers, L. R.; Dahl, L. F. *Inorg. Chem.* **1980**, *19*, 680–692.
(29) Smith, A. E. *Inorg. Chem.* **1972**, *11*, 165–170.
(30) Mitschler, A.; Rees, B.; Lehmann, M. S. *J. Am. Chem. Soc.* **1978**, *100*, 3390–3397.
(31) Day, V. W.; Reimer, K. J.; Shaver, A. *J. Chem. Soc., Chem. Commun.* **1975**, 403–404.
(32) Dahl, L. F.; Wei, C. H. *Inorg. Chem.* **1963**, *2*, 713–721.
(33) Guggenberger, L. J.; Cramer, R. *J. Am. Chem. Soc.* **1972**, *94*, 3779–3786. Fitzpatrick, P. J.; LePage, Y.; Sedman, J.; Butler, I. S. *Inorg. Chem.* **1981**, *20*, 2852–2861.
(34) Seiler, P.; Dunitz, J. *Acta Crystallogr., Sect. B* **1980**, *B36*, 2255–2260.
(35) Takusagawa, F.; Koetzle, T. F. *Acta Crystallogr., Sect. B* **1979**, *B35*, 1074–1081.
(36) Zimmerman, G. J.; Sneddon, L. G. *Inorg. Chem.* **1980**, *19*, 3650–3655.
(37) Ibers, J. A. *J. Organomet. Chem.* **1974**, *73*, 389–400.
(38) Rees, B.; Coppens, P. *Acta Crystallogr., Sect. B* **1973**, *B29*, 2516–2528.
(39) Hodgson, K. O.; Raymond, K. N. *Inorg. Chem.* **1973**, *12*, 458–466. Jemmis, E. D.; Alexandratos, S.; Schleyer, P. v. R.; Streitwieser, A. J.; Schaefer, H. F. *J. Am. Chem. Soc.* **1978**, *100*, 5695–5700.

Table VI. Valence Orbitals from the SCC-DV-Xα Calculation of $(\eta^5\text{-}C_5H_5)Co(HN_4H)$

		major percent atomic compositions[a]			
orbital	energy, eV	Co	N_2H_2	N_2	$\eta^5\text{-}C_5H_5$
19 a″	−1.547		26 (pπ)	71 (pπ)	
18 a″	−3.097	34 (d_{xy})	17 (pσ), 7 (2s)		38
30 a′	−4.568	36 (d_{xz})	29 (pπ)	11 (pπ)	23
29 a′[b]	−6.738	80 (d_{z^2}), 7 (s)			7
17 a″	−6.934	64 (d_{yz})	21 (pπ)	11 (pπ)	
28 a′	−7.052	20 (d_{xz})	33 (pπ)	23 (pπ)	19
27 a′	−7.320	85 ($d_{x^2-y^2}$)			5
16 a″	−7.712		17 (pσ)	20 (s), 34 (pσ)	23
15 a″	−8.406	15 (d_{xy})		5 (s), 15 (pσ)	59
26 a′	−8.998	6 (s)	20 (pσ)	54 (pσ)	
14 a″	−9.069	24 (d_{yz})	64 (pπ)	9 (pπ)	
25 a′	−9.231	27 (d_{xz})			66
13 a″	−10.442	5 ($4p_y$)			84
24 a′	−10.804				97
23 a′	−11.551		31 (pπ)	63 (pπ)	
22 a′	−11.844		5 (pσ)		84
12 a″[c]	−11.851	24 (d_{xy})	7 (2s), 48 (pσ)		10
11 a″	−12.960				96
21 a′	−13.588		51 (pσ)	23 (pσ)	17
20 a′	−13.670				90

[a] 5% or greater, pσ denotes in xy plane pπ = p_z orbitals with the coordinate system defined in the text. [b] Highest filled orbital. [c] 6% H 1s.

Table VII. Comparison of Metallacycle π Orbitals in $(\eta^5\text{-}C_5H_5)Co(HN_4H)$ and $Fe(CO)_3(HN_4H)$

cobalt complex					iron complex				
		atomic composition[a]					atomic composition[a]		
orbital	energy, eV	Co	N_2H_2	N_2	orbital	energy, eV	Fe	N_2H_2	N_2
19 a″	−1.547		26	71	23 a″	−2.243		22	63
30 a′	−4.568	36 (d_{xz})	29	11	32 a′	−5.133	29 (d_{xz})	22	16
17 a″	−6.934[b]	64 (d_{yz})	21	11	18 a″	−7.936	41 (d_{yz})	18	7
28 a′	−7.052	20 (d_{xz})	33	23	31 a′[b]	−7.621	28 (d_{z^2})	21	14
14 a″	−9.069	24 (d_{yz})	64	9	16 a″	−9.700	9 (d_{yz})	64	9

[a] Percent compositions and only the N_2H_2 and N_2 pπ contributions are given. [b] Highest occupied π orbital.

visible spectrum, deriving its color from an intense ultraviolet absorption that tails into the visible region. Note that the band maxima (Table V) are essentially insensitive to solvent polarity, thereby ruling out a simple metal to ligand π* charge-transfer assignment, as found in certain diazabutadiene complexes.[40] An n → π* transition (involving the remote nitrogen lone pairs) may be eliminated from consideration owing to lack of a solvent effect and the high intensities.[41]

While structural data for complex IVc rule out strong conjugation between the metallacycle and phenyl rings owing to noncoplanarity, the energies of the electronic transitions show some sensitivity to the phenyl substituents. The energy difference between λ_{max}^1 and λ_{max}^2 remains essentially constant for all groups. Replacing methyl substituents by aromatic groups leads to a systematic red shift of all three absorption bands, as expected if these transitions involve the metallacycle π network. Extension of the conjugated network, in this case partial conjugation between the metallacycle and phenyl rings, stabilizes the excited state, resulting in a bathochromic shift. Increased substitution of fluorine atoms for hydrogen atoms on the phenyl rings has little effect on λ_{max}^1 and λ_{max}^2, while λ_{max}^3 undergoes a gradual hypsochromic shift.

Molecular Orbital Models. In order to understand better the π interactions between the metal d orbitals and the tetraazadiene chelate, we performed SCC-DV-Xα calculations on $(\eta^5\text{-}C_5H_5)Co$, HN_4H, and $(\eta^5\text{-}C_5H_5)Co(HN_4H)$ (Figure 5). For a more complete listing of the molecular valence orbitals and their atomic composition see Table VI. The key interaction between the occupied 21 a′ d_π orbital of the $(\eta^5\text{-}C_5H_5)Co$ fragment and the empty 9a′ π* orbital of the tetraazadiene ligand produces the metallacycle π-bonding orbital 28 a′ and its antibonding counterpart 30 a′. Partial occupation[42] of the 9 a′ tetraazadiene orbital, which exhibits nodal pattern A explains

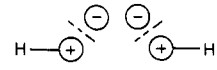

A

the lengthening of the N(1)–N(2) and N(4)–N(3) bonds and shortening of the N(2)–N(3) distance in complex IVc. The lower occupied 14 and 17 a″ orbitals in $(\eta^5\text{-}C_5H_5)Co(HN_4H)$ contain contributions from HN_4H pπ orbitals with nodal pattern B. As expected, the most stable metallacycle π orbital (23 a′) contains ligand character of the type

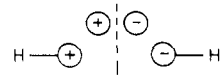

B

(40) Bock, H.; tom Dieck, H. *Chem. Ber.* **1967**, *100*, 228–246.
(41) Albini, A.; Kisch, H. *Top. Curr. Chem.* **1976**, *65*, 105–145.

(42) A reviewer suggested that, because the energy of 9 a′ is less than 21 a′, the complex is a cobalt(III) derivative. This viewpoint is oversimplified, because as negative charge flows into 9 a′ (when the complex is formed), it will destabilize 9 a′. The positive charge that develops on the $(\eta^5\text{-}C_5H_5)Co$ fragment will stabilize 21 a′. A population analysis reveals a 0.51+ charge develops on the $(\eta^5\text{-}C_5H_5)Co$ fragment and a 0.51− charge develops on the HN_4H fragment in the molecule. The charge on Co is 1.40+ from this analysis.

C and the most unstable type (19 a″) exhibits the maximum number of nodes D. Only the empty ligand orbital

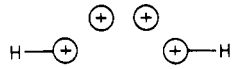

C

D

A and the filled ligand orbital B appreciably interact with cobalt d_{xz} and d_{yz} orbitals, respectively (Table VI and coordinate system as defined in Figure 5). Ligand types A and B, correspond to the 9 a′ and 6 a″ orbitals of Figure 5.

A comparison of the interactions between the isoelectronic $(\eta^5\text{-}C_5H_5)Co$ and $Fe(CO)_3$ fragments with π orbitals of an HN_4H fragment is provided in Table VII. Although general π-orbital splittings and their compositions are similar for the two complexes, the percent tetraazadiene π^* (type A) character differs for 28 a′ and 31 a′ in the cobalt and iron complexes, respectively. Greater contribution from the ligand π^* orbital in the cobalt case leads to increased back-bonding compared with $Fe(CO)_3(HN_4H)$. The iron d_{z^2} character found in 31 a′ is also noteworthy since this orbital cannot effectively overlap with the tetraazadiene π^* orbital. This could explain the nearly fivefold increase in intensity of the metallacycle $\pi \rightarrow \pi^*$ transition (vide infra) in the cobalt complexes, since cobalt employs d_{xz} orbital character in 28 a′.

Transition-state calculations[43] place the lowest one-electron transition of $(\eta^5\text{-}C_5H_5)Co(HN_4H)$ at 2.38 eV, and the electronic spectrum of $(\eta^5\text{-}C_5H_5)Co(CH_3N_4CH_3)$ exhibits a weak feature (Figure 4) at 598 nm (2.07 eV). The weak intensity arises from lack of overlap between the d_{z^2} orbital, 29 a′, and the π^* orbitals of the N_4 ring. Although three other transitions, 17 a″, 28 a′, and 27 a′ → 30 a′ should lie at slightly higher energies, only two other transitions are apparent (Figure 4). We attribute the most intense band at 424 nm to the $\pi \rightarrow \pi^*$ excitation localized on the metallacycle (28 a′ → 30 a′). Calculations may incorrectly estimate the energy of 17 a″ → 30 a′, or this transition could be hidden beneath the intense 424-nm feature. Just as for the iron(0) tetraazadiene complex,[2a,b] the vivid colors of the cobalt(I) tetraazadiene compounds may be attributed to the low-lying unoccupied metallacycle π^* orbital.

Acknowledgment. We thank the National Science Foundation for support of this work (Grants CHE 78-01615 and 81-05069 to W.C.T. and CHE 80-09671 to J.A.I.).

Registry No. IVa, 80738-16-5; IVb, 76418-81-0; IVc·$^1/_2C_6H_6$, 80738-17-6; IVd, 80738-18-7; IVe, 80738-19-8; $(\eta^5\text{-}C_5H_5)Co(HN_4H)$, 80738-20-1.

Supplementary Material Available: Tables of the positional and thermal parameters, of the root-mean-square amplitudes of vibration, and a listing of observed and calculated structure amplitudes (22 pages). Ordering information is given on any current masthead page.

(43) Slater, J. C. "The Self-Consistent Field for Molecules and Solids"; McGraw-Hill: New York, 1974.

5,6:11,12-Bis(ditelluro)tetracene: Synthesis, Molecular, and Supramolecular Properties[1]

Daniel J. Sandman* and James C. Stark†

GTE Laboratories, Waltham, Massachusetts 02254

Bruce M. Foxman*

Department of Chemistry, Brandeis University, Waltham, Massachusetts 02254

Received December 2, 1981

5,6:11,12-Bis(ditelluro)tetracene (5,6,11,12-tetratellurotetracene, TTeT), synthesized in 13% yield from 5,6,11,12-tetrachlorotetracene and a new sodium ditelluride reagent, absorbs at longer wavelengths in both solution and solid state and is oxidized electrochemically at a lower potential, compared to its selenium analogue. The structure of TTeT, a monoclinic crystal (a = 11.746 (4) Å, b = 4.364 (2) Å, c = 15.831 (5) Å, β = 90.57°, space group $P2_1/n$, R = 0.030, R_w = 0.037), exhibits short interstack contacts of 3.701 (1) Å.

The organoselenium π donors which give ion-radical solids with metallic states below 30 K are 5,6:11,12-bis(diseleno)tetracene **1** (TSeT)[2] and derivatives of tetraselenafulvalene (TSeF, **2**), and ambient pressure superconductivity has been observed to date only in the 2:1 perchlorate salt of the tetramethyl derivative of **2**.[3] Substitution of tellurium for selenium in **1** and **2** is expected

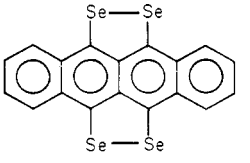

1

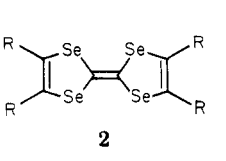

2

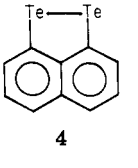

4

†On sabbatical leave at GTE Laboratories, 1980–1981, from the Department of Chemistry, Eastern Nazarene College, Quincy, MA 02170. This work was supported in part by National Science Foundation Grant SP1-8160202.

0276-7333/82/2301-0739$01.25/0